Journal of Materials Processing Technology 212 (2012) 633–639

Contents lists available at SciVerse ScienceDirect

Journal of Materials Processing Technology

journal homepage: www.elsevier.com/locate/jmatprotec

Glass biochip fabrication by laser micromachining and glass-molding process

Chien-Yao Huang[a,b,*], Chao-Hui Kuo[a], Wen-Tse Hsiao[a], Kuo-Cheng Huang[a], Shih-Feng Tseng[a,b], Chang-Pin Chou[b]

[a] Instrument Technology Research Center, National Applied Research Laboratories, Hsinchu 300, Taiwan
[b] Department of Mechanical Engineering, National Chiao Tung University, Hsinchu 300, Taiwan

ARTICLE INFO

Article history:
Received 9 March 2011
Received in revised form 18 July 2011
Accepted 14 October 2011
Available online 20 October 2011

Keywords:
Laser micromachining
Precision glass molding
Micro channel
Biochip
Glass

ABSTRACT

Due to their low cost, small size, and high-speed performance, biochips are often used in various bio-experiments. Compared with polymer-based biochips, glass-based substrates are less sensitive to heat and organic environments. This study presents a hybrid processing approach that uses laser micromachining (LMM) and precision glass molding (PGM) techniques to mass-produce glass-based biochips. A silicon carbide (SiC) mold with an outside diameter of 20 mm was used to hot emboss biochip channels measuring 200 μm wide and 185 μm deep. This study also identifies the optimal conditions for glass molding when processing soda-lime glass for biochip applications, and discusses the influence of the major processing parameters on biochip channel depth. This study uses the Taguchi method to assess the effects of several molding parameters on larger-the-better performance characteristics. The experiments in this study consider the effects of several molding parameters, such as molding temperature, pressing force, moving speed, temperature holding time, and vacuum environment, to achieve optimum characteristics for biochip channels. Orthogonal array analysis indicates that the optimal process parameters includes a 620 °C molding temperature, 1 kN pressing force, 5 mm/min moving speed, 60 s temperature holding time, and a vacuum-free environment. This study also investigates the surface roughness of glass biochip channels.

1. Introduction

Biochips combine advanced micro electro mechanical systems (MEMS) and optoelectronic techniques. Biochips are smaller, lighter, and cheaper than traditional instruments. As a result, biochips offer more advantages than traditional experimental methods without biochips, improving efficiency and reducing sample consumption. Biochips are usually made out of polymer materials, such as polydimethylsiloxane (PDMS) and polymethylmethacrylate (PMMA), but these polymer materials are not suitable for all organic environments. Compared with the polymer-based biochips, glass-based substrates have better heat tolerance, thermal stability, and chemical stability, and are suitable for organic environment and wide-spectrum transmission. Therefore, glass-based biochips have been widely used in bio-experiments.

Some literatures presented several methods for fabricating glass materials, including LMM, CNC milling, ultra-precision diamond turning, ultrasonic vibration machining, chemical wet etching, and precision glass molding (PGM) as summarize in the following: Cheng et al. (2005) developed a debris-free laser direct-writing method to fabricate glass chip. In this approach, the overall development time is within hours, but the cross-sectional profile of biochip bottom is circular not rectangular, and the biochip channels are less than 100 μm wide or deep. Yuen et al. (2000) employed a CNC milling pyrexglass microvalve in a totally integrated microfluidics system to analyze sample preparation, biochemical reaction, and detection/quantitation steps for DNA analyses. Although a CNC machined microvalve system is easy to fabricate and does not require a clean-room, the minimum width of the biochip channels it can produce is limited by the diameter of the end mill. Moriwaki et al. (1992) used ultrasonic vibration to achieve the ultraprecise ductile cutting of soda-lime glass. The grooving experiments in their study showed that this method increased the critical depth of the cut for ductile cutting and transferred the surface profile of the diamond cutting edge to the cut groove compared to the conventional cutting. Liu et al. (2005) evaluated the cutting performance of soda-lime glass using an ultra-precision lathe with a single-crystal diamond tool. Their experimental results indicate that ductile cutting can be achieved when the undeformed chip thickness is less than a critical value. Even if ultra-precision diamond grinding and ultrasonic vibration machining can manufacture glass, they are slow processes. In these methods, the surface

* Corresponding author at: Instrument Technology Research Center, National Applied Research Laboratories, Hsinchu 300, Taiwan. Tel.: +886 3 5779911x636; fax: +886 3 5773947.
E-mail address: msyz@itrc.narl.org.tw (C.-Y. Huang).

0924-0136/$ – see front matter © 2011 Elsevier B.V. All rights reserved.
doi:10.1016/j.jmatprotec.2011.10.013

profiles are limited by tools, which wear out over time. Matsumura and Ono (2008) discussed a cutting process using ball end mills for machining microgrooves on glass. Orthogonal grooves 15–20 μm deep and 150–175 μm wide were machined in a feed of the cutter for each groove, achieving crack-free glass milling. However, like the ultra-precision diamond grinding and ultrasonic vibration machining methods, the surface profiles are limited by tools and milling wears out the tools. Iliescu et al. (2007) fabricated a through hole in 500 μm thick Pyrex glass wafer using chemical wet etching. Iliescu et al. (2008) presented and analyzed the main factors contributing to the wet etching of Pyrex glass. One problem of the chemical wet etching is that chemical solutions, such as HF solution, cause environmental pollution. Tsai et al. (2008) confirmed the feasibility of the elasto-viscoplastic model for glass based on the molding temperature. This model can be used in the FE analysis of the prediction and modification of properties of the final lens products. Yan et al. (2009) used microstructure arrays as molds for hot-press glass molding experiments and achieved good geometrical transferability. Zhou et al. (2010) investigated the manufacture of aspherical lenses using the glass molding technique. Experimental and simulation results show that a nonisothermal glass molding press is an effective way to improve the molding efficiency of dies and prolong their service life. The glass molding technique is an ideal process for mass-production, but the mold, usually made by precision diamond grinding technique, is very expensive.

This study presents a hybrid processing approach that combines laser micromachining (LMM) and precision glass molding (PGM) techniques to mass-produce glass-based biochips. The advantages of LMM are its small processing dimensions (30 μm), short processing time, and lower cost than the precision diamond grinding technique. This study uses the Taguchi method to assess the effects of several molding parameters on performance. This paper also determines the effects of several molding parameters, such as molding temperature, pressing force, moving speed, temperature holding time, and vacuum-free environment, on the optimum biochip channel characteristics. This study also discusses the surface roughness of glass biochip channels.

2. Experiment details—micro-channels fabrication

2.1. Mold materials

The molds used in glass molding processes must have high stiffness and no adhesion characteristics. As a result, common materials for these molds include stainless steel, silicon carbide (SiC), tungsten carbide (WC), and glassy carbon (GC). After the LMM of micro-channels for glass molding processes, the surface exhibits residual metal particles and recasting regions of metal based substrates, such as WC and stainless steel. Fig. 1 shows recasting regions and residual metal particles of WC and SiC materials after LMM processing.

Table 1
The thermal properties of SiC.

Properties	Silicon carbide
Density (g/cm^3)	3.21
Melting point (°C)	2730
Thermal conductivity (W/(cm K))	3.6

Table 2
The properties of soda-lime glass.

Properties	Soda-lime glass
Glass transition temperature, T_g (°C)	573
Coefficient of thermal expansion (ppm/K), ~100–300 °C	9
Refractive index at 20 °C (n_D)	1.518
Dispersion at 20 °C, 104 × ($n_F - n_C$)	86.7

Compared with two types mold material, the SiC has uniform surface due to material structure is powder sinter. Therefore, this study adopts a SiC mold. Table 1 summarizes the thermal properties of SiC materials, as described by Park (1998). Commercial soda-lime glass substrate is much cheaper than other types of glass, and is used in many bio-experiments. Table 2 lists the properties of commercial soda-lime glass, as described by Seward and Vascott (2005). The transition temperature (T_g) of commercial soda-lime glass is 573 °C, making it easy to form biochips using the PGM processes.

2.2. Hybrid processing methods

2.2.1. Laser micromachining (LMM)

SiC material is a brittle and non-conductive material. Thus, it is difficult to process SiC using traditional mechanical methods such as end mill milling and electrical discharge machining (EDM). In additional, due to SiC's high absorption of laser wavelength and high pulse energy, the LMM technique can quickly fabricate various structures on the mold's surface. Lau et al. (1995) proposed that laser was effective tools in shaping composite materials which has peculiar properties including anisotropy, low thermal conductivity and the abrasive nature of the reinforcing phases. Liu et al. (2011) proposed that laser drilling produces much higher etch rates than conventional dry etching in SiC substrates by UV laser. Because of these fabrication advantages, the experiments in this study used the LMM process to fabricate the biochip structure on SiC material for PGM processes. Fig. 2 illustrates the LMM system. An AVIA 355-14 ultraviolet (UV) laser system with wavelength of 355 nm was adopted in this study. Table 3 shows the specifications of the UV laser system.

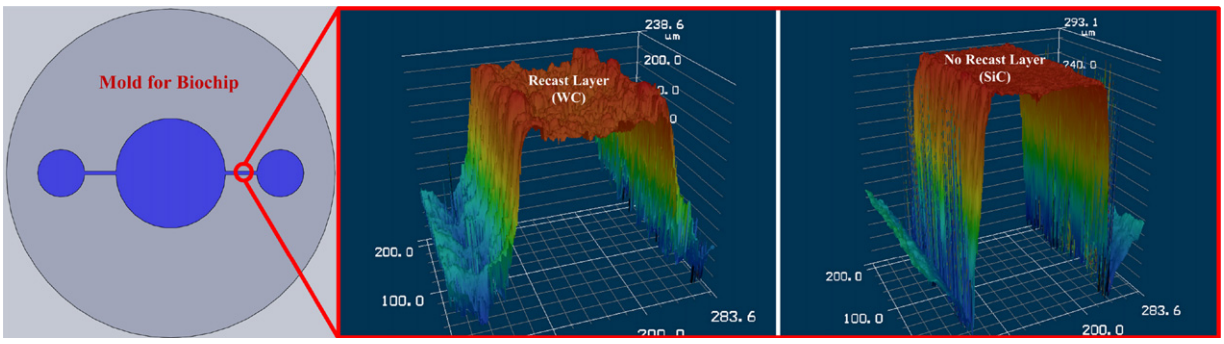

Fig. 1. Profile of mold (after LMM).

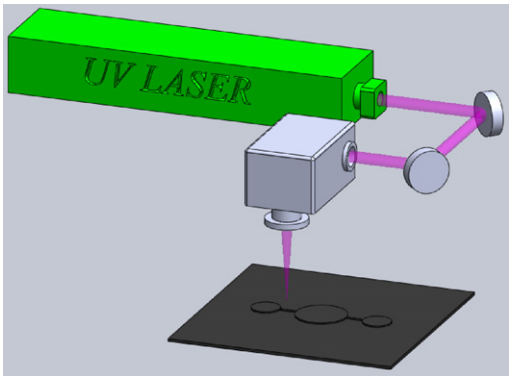

Fig. 2. Sketch of laser micromachining.

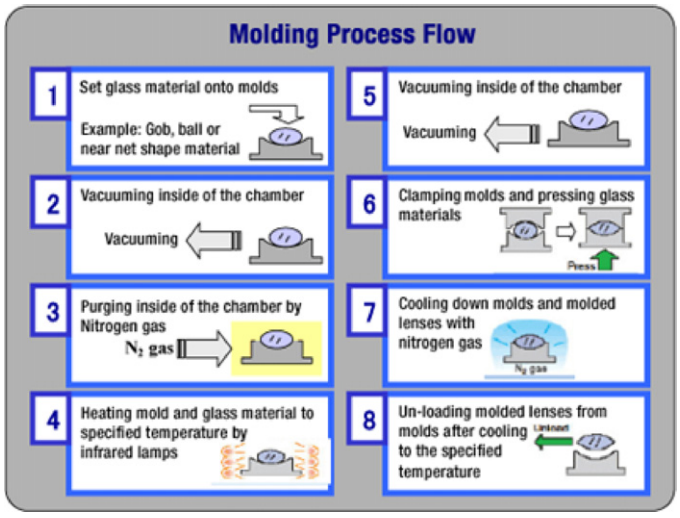

Fig. 3. PGM processing.
Cited from Toshiba (2011).

2.2.2. *Precision glass molding (PGM)*

The precision glass molding process involves heating glass material above the transition temperature and using a precise

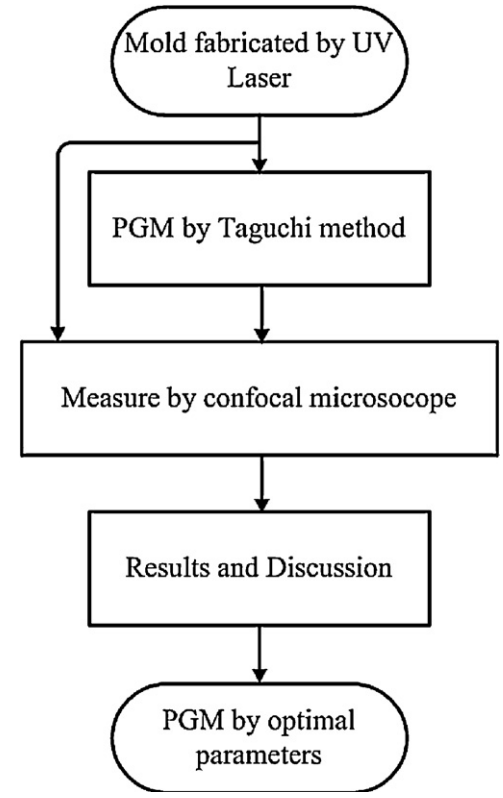

Fig. 4. Flowchart of experiment.

Table 3
Specification of the UV laser system.

1. Wavelength	355 nm
2. Pulse repetition rate range	≧100 kHz
3. Average power @ 100 kHz	>10 W
4. Pulse width @ 100 kHz	≦40 ns
5. Spatial mode	TEM00
6. Beam quality factor, M^2	≦1.3

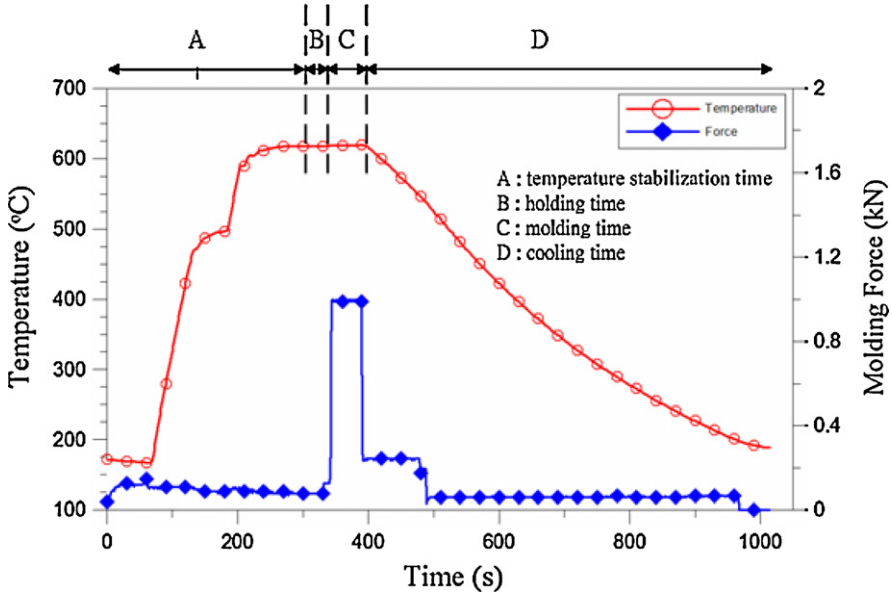

Fig. 5. Temperature and force of PGM process with respect to cycle time.

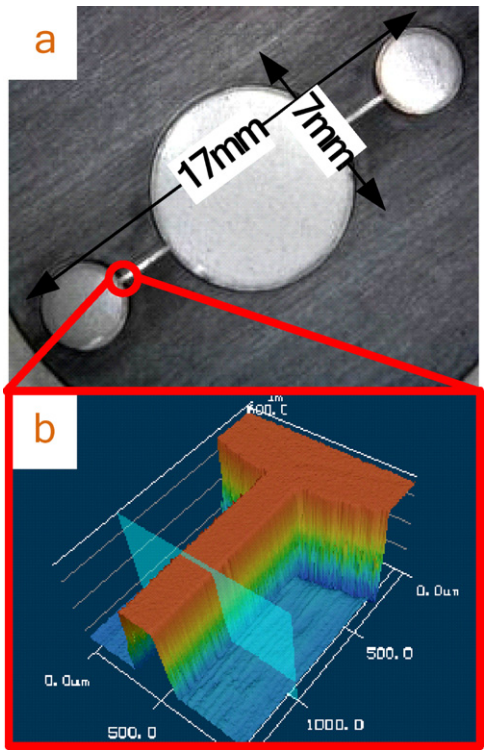

Fig. 6. Structure of mold on SiC. (a) Optical photo and (b) 3D profile.

hot-embossing method to form the glass components. The PGM process has several advantages, including a short cycle time for molding processes, high accuracy, and high freedom for components profile. High-precision molding allows the mass-production of high-quality optical components. The experiments in this study used a GMP-207-HV (Toshiba Machine Co. Ltd.) optical glass mold press machine for PGM. Fig. 3 is a flowchart of the PGM process, cited from Toshiba (2011). The steps of PGM processing are illustrated as follows:

(a) Loading glass material onto mold.
(b) Vacuuming inside of the chamber.
(c) Purging inside of the chamber by nitrogen gas.
(d) Heating mold and glass material to specified temperature by infrared lamps.
(e) Vacuuming inside of the chamber.
(f) Clamping molds and pressing glass material.

Table 4
Factors and levels for glass molding process.

Control factor	Level 1	Level 2	Level 3	Level 4
Temperature (°C)	590	600	610	620
Pressing force (kN)	0.4	0.6	0.8	1.0
Speed (mm/min)	5	10	15	20
Temperature holding time (s)	20	40	60	80
Vacuum environment	Without		With	

Table 5
Parameters of LMM.

Parameter	Value
Laser power	8.8 W
Pulse width	8 μs
Frequency	70 kHz
Speed	2000 mm/s
Machining path	Crosshatch and bidirectional
Passes	60

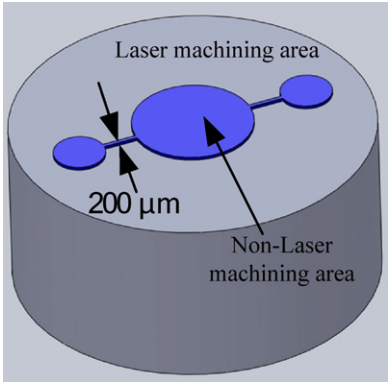

Fig. 8. Sketch of laser machining area.

(g) Cooling down molds with nitrogen gas.
(h) Un-loading molded samples from molds after cooling to the specified temperature.

2.2.3. Optimization performance characteristics—Taguchi method

This study uses the Taguchi method to assess the effects of several molding operational parameters on the larger-the-better performance characteristics. The Taguchi method is a useful tool for designing quality systems, as it provides a simple, efficient, and systematic approach to optimize performance, quality, and cost. Taguchi parameter design can optimize performance by adjusting

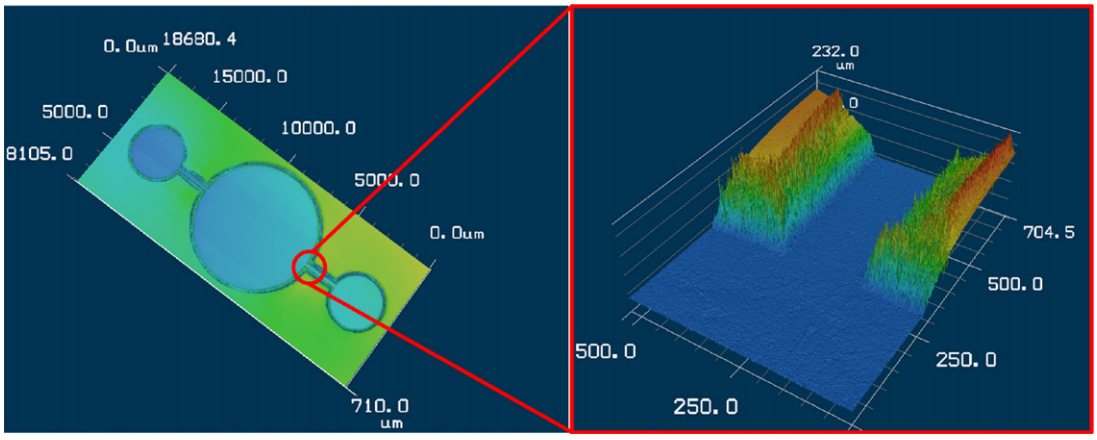

Fig. 7. Experimental results of micro channel structure on soda-lime glass.

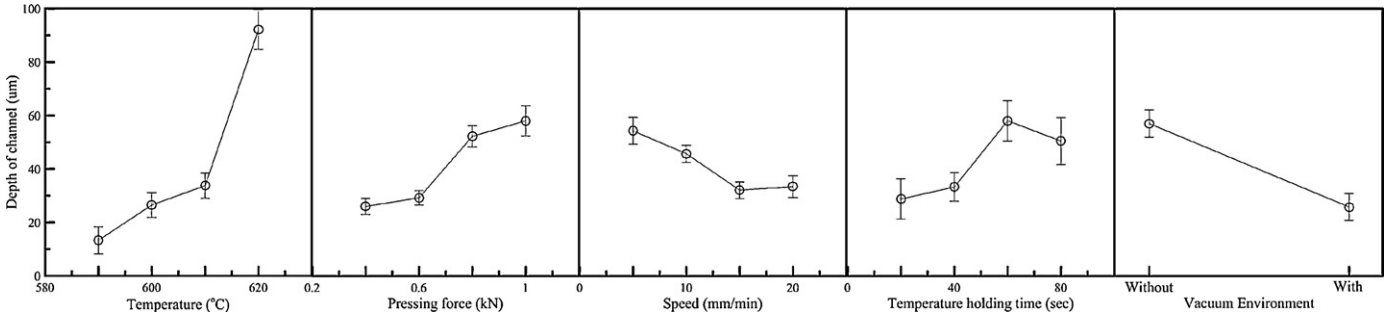

Fig. 9. The results of Taguchi method.

design parameters and reducing the sensitivity of the system performance to sources of variation, as described by Yang and Tarng (1998) and Ghani et al. (2004). Orthogonal arrays based on the Taguchi method can determine the effect of several parameters.

To reduce crack phenomenon of the molding processes on glass substrates, the molding temperature was set above the soda-lime glass transfer temperature (573 °C). In this case, the molding temperature varied from 590 to 620 °C. If the temperature exceeded 620 °C during the PGM heating step, soda-lime glass broke easily. Exceeding the pressing force also caused the glass substrates to crack. Therefore, the range of pressing force was set from 400 to 1000 N in this experiment. After an initial experiment to decide the range of factors, the levels of control factors are shown in Table 4.

3. Experimental

Fig. 4 is a flowchart of the experiment. The diameter of the silicon carbide mold used to hot emboss the biochip was 20 mm. The micro structure was formed on the SiC surface using LMM processing. Table 5 shows the experimental parameters of LMM. After the LMM process, the surface profile and microstructure of mold were measured by three dimensional confocal microscopes (KEYENCE, VK-9700). The SiC mold was then used to fabricate glass based biochips using the Taguchi method and PGM. This study also analyzes the effects of PGM processing parameters, such as molding temperature, pressing force, moving speed, temperature holding time, and vacuum environment.

Fig. 5 shows the relationships between temperature and molding pressing force for PGM process with respect to cycle time. The molding process includes four steps: (A) temperature stabilization time, (B) holding time, (C) molding time, and (D) cooling time. After the temperature stabilization time, the temperature of mold and preform achieved the setting temperature. The holding time increased as the preform size increased, leading to a more uniform temperature. In the molding time, the machine presses the preform to form the profile. The cooling time proceeds until the component cools to 200 °C. One cycle time of PGM process was approximately 17 min for biochip fabrication.

4. Analysis results and discussion

Fig. 6 shows the mold profile measurement results by confocal microscope. The micro-structure profile of the mold was readily apparent after laser machining. Fig. 7 shows the profile of the biochip micro channel structure on soda-lime glass after PGM processing. These experimental results reveal a uniform bottom and vertical side.

The quality of the biochip was evaluated in terms of surface roughness and geometric dimensions. The flow rate and volume of bio-samples in bio-experiments depended on the dimensions of the micro channels. Accurate micro channel dimensions in a

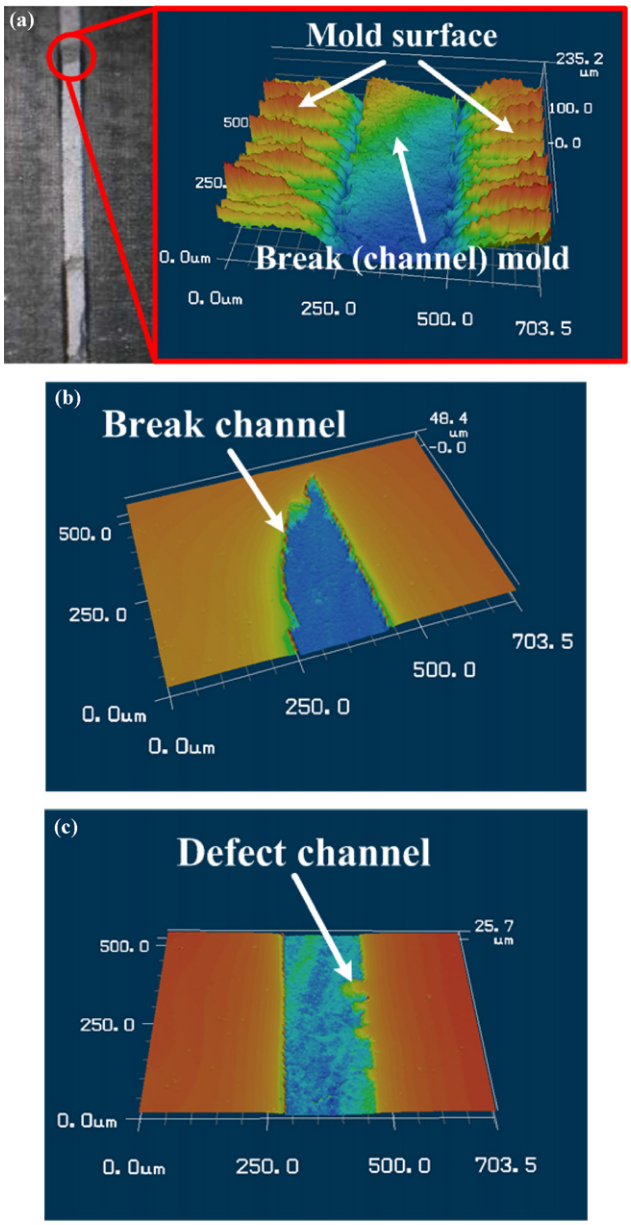

Fig. 10. Break mold and defect channels. (a) Break mold, (b) break channel on glass and (c) defect channel.

biochip can increase experimental accuracy, and a smooth surface can avoid residual bio-samples. During PGM processing, the surface roughness of the biochip depends on the SiC mold. In this study, the roughness of the mold was 0.7 μm (Ra). After PGM processing, the

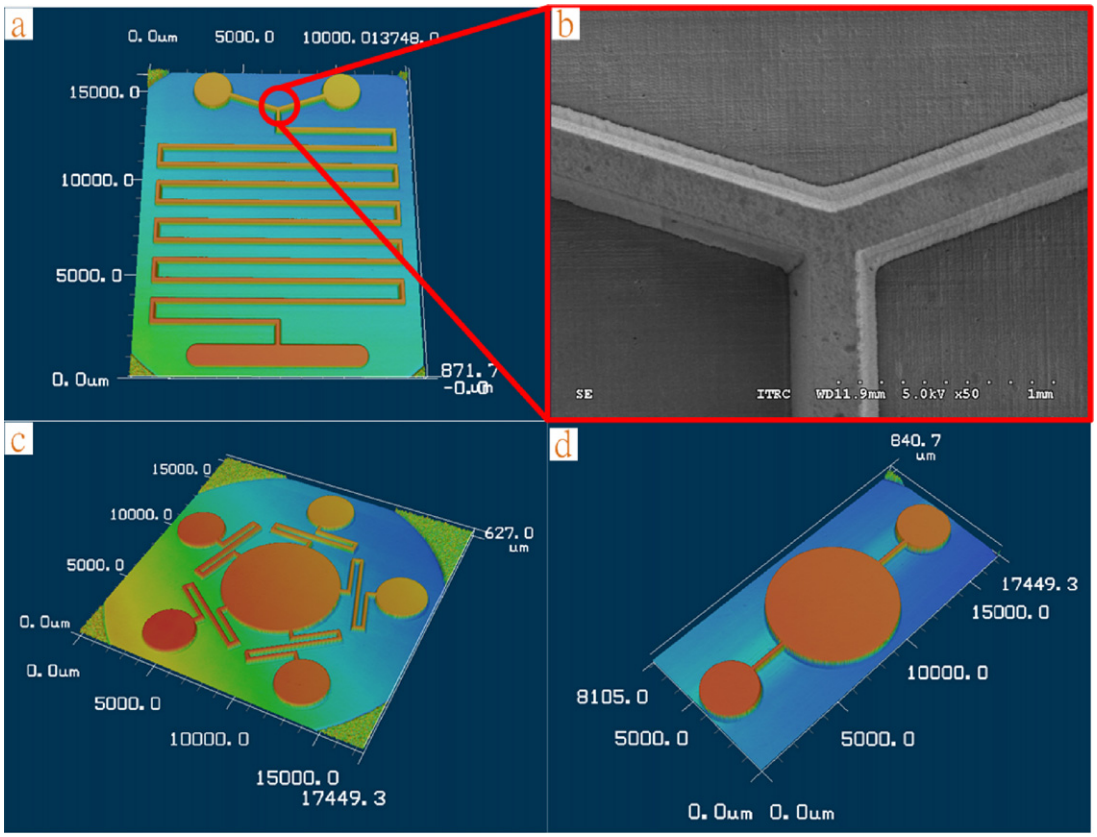

Fig. 11. SiC molds measured by confocal microscope and SEM.

average roughness of soda-lime glass surface was 0.73 μm (Ra) and standard deviation is 0.035 μm. Fig. 8 shows a sketch of the laser machining area. The protruding structure in this figure is the non-laser machining area, showing that the surface roughness depends on the initial SiC surface roughness. The depth of the biochip channels depended on the fill rate, which in turn is related to stable PGM process.

This study uses Taguchi orthogonal array analysis to determine the relationship between with PGM parameters and biochip channel depth. Fig. 9 plots these relationships. Because the liquidity of glass increases at higher temperatures, it is easy to form the biochip. However, exceeding molding temperature leads to the crack phenomenon, as Fig. 10 shows. Residual stresses fractured the soda-lime glass; therefore, the molding pressing force could not exceed 1000 N. Due to lager force can against lager resistance of glass to get deeper channel during PGM processing. When the force below 1000 N, increasing force leads more depth channel.

In PGM processing, the moving speed also affect the channel depth: the depth increases as the speed decreases. Because the moving speed increasing causes faster deformation of glass, the flow-ability of glass decreases. Fig. 9 shows the optimum moving speed for obtaining the maximum depth was 5 mm/min. A longer temperature holding time was necessary to obtain a uniform temperature and decrease cracking during the molding process. However, excessive time caused the energy waste and let channel depth unstable. To evaluate the error bar in Fig. 9, the optimum temperature holding time was set at 60 s. The molding machine using in this research fills nitrogen gas when the setting is vacuum-free environment. Therefore, the heating method includes convection not only radiation and conduction. So the vacuum-free environment obtained deeper biochip channels. Fig. 9 also shows that the temperature is more important than other parameters, while speed is the least important.

Fig. 10 shows a picture of the mold when the overloading temperature or force of PGM processes breaks the SiC mold. Fig. 10(a) shows the break of mold, and (b) depicts micro channels formed with a defective mold. After repeated molding, the SiC mold which is the powder sinter will fall off; in this case, the bottoms and sides of channels produce disproportionate surface, as Fig. 10(c) shows.

The Taguchi method can predict experimental results with optimal parameters. An analysis of Fig. 9 shows that the optimal parameters are level 4 for temperature, level 4 for pressing force, level 1 for speed, level 3 for temperature holding time, and level 1 for vacuum environment. Table 6 lists the optimal parameter settings, where T is temperature (°C), P is pressing force (kN), V is speed (mm/min) and Vac is assisted vacuum of PGM processing.

The following formula predicts experiment result:

$$D = A + (Te4 - A) + (P4 - A) + (V1 - A) + (HT3 - A) + (Va1 - A)$$

where D is the optimal depth of the biochip channels, A is the average of Taguchi orthogonal array results, $Te4$ is level 4 temperature,

Table 6
Optimum parameters.

T (°C)	P (kN)	V (mm/min)	Holding time (s)	Vac.	Depth (μm)
620	1	5	60	Without	185.68

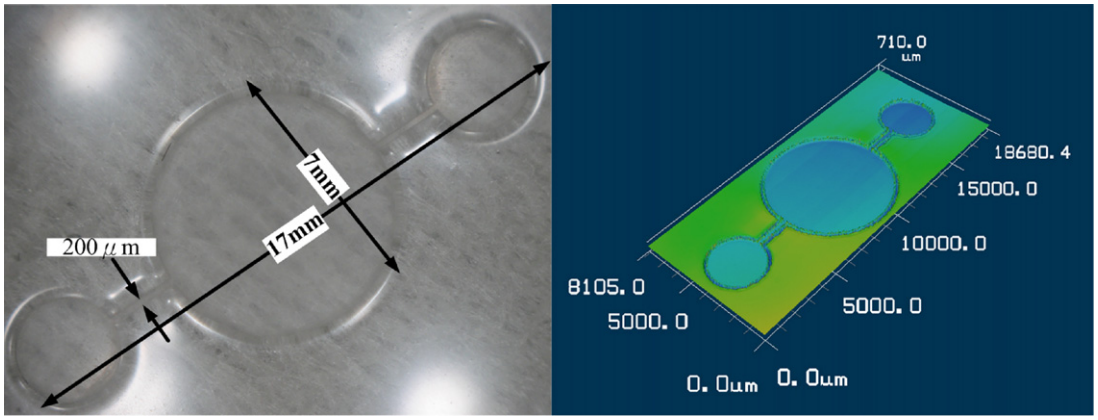

Fig. 12. Glass biochip.

*P*4 is level 4 pressing force, *V*1 is level 1 speed, *HT*3 is level 3 holding time, and *Va*1 is level 1 vacuum environment.

The Taguchi orthogonal array and results of PGM experiments show that the average Taguchi orthogonal array results are as follows:

$$A = \frac{12.96 + 13.8 + 17.53 + 8.88 + 14.89 + 17.38 + 33.25 + 40.57 + 29.62 + 45.1 + 32.18 + 28.12 + 46.72 + 40.9 + 126.3 + 154.85}{16}$$

$$= 41.44$$

Therefore, the optimal biochip channel depth can be obtained as follows:

$$D = A + (Te4 - A) + (P4 - A) + (V1 - A) + (HT3 - A) + (Va1 - A)$$

$$= 41.44 + (50.75 - 41.44) + (16.66 - 41.44) + (12.90 - 41.44) + (16.65 - 41.44) + (15.61 - 41.44) = 154.03$$

Table 6 shows the optimal parameter settings for PGM processing based on the Taguchi method. The biochip channel depth was 185 μm, which was deeper than predicted, because the depth of biochip increased quickly above 610 °C.

The bio-experiments are various types, and diverse functions lead different design patterns of biochip. The LMM method can quickly and easily fabricate various patterns on a mold. Fig. 11 shows various SiC biochip molds made by LMM. Fig. 12 shows a glass biochip measuring 7 mm wide and 17 mm long. The biochip channel measured 200 μm wide and 185 μm deep. Since biochip micro channels are generally smaller than 200 μm, the results of this paper are applicable to biochip channels.

5. Conclusion

Micro structures were fabricated on a SiC mold using LMM, and this mold was then used to form biochips through the PGM process. This study uses the Taguchi method to determine the optimal parameter settings. Taguchi orthogonal array results show that the optimal parameters included a 620 °C temperature, 1 kN pressing force, 5 mm/min speed, 60 s temperature holding time, and a vacuum-free environment. These optimal parameters formed micro channels measuring 200 μm wide and 185 μm deep, with a surface roughness of 0.7 μm (Ra). The micro channels were formed on glass biochips measuring 7 mm wide and 17 mm long. In the future, structures such optical elements could be combined with glass biochips to increase their usefulness and versatility.

References

Cheng, J.Y., Yen, M.H., Wei, C.W., Chuang, Y.C., Young, T.H., 2005. Crack-free direct-writing on glass using a low-power UV laser in the manufacture of a microfluidic chip. Journal of Micromechanics and Microengineering 15, 1147–1156.
Ghani, J.A., Choudhury, I.A., Hassan, H.H., 2004. Application of Taguchi method in the optimization of end milling parameters. Journal of Materials Processing Technology 145, 84–92.
Iliescu, C., Chen, B., Miao, J., 2008. On the wet etching of Pyrex glass. Sensors and Actuators A: Physical 143, 154–161.
Iliescu, C., Tay, F.E.H., Miao, J., 2007. Strategies in deep wet etching of Pyrex glass. Sensors and Actuators A: Physical 133, 395–400.
Lau, W.S., Yue, T.M., Lee, T.C., Lee, W.B., 1995. Un-conventional machining of composite materials. Journal of Materials Processing Technology 48, 199–205.
Liu, L., Chang, C.Y., Wu, W., Pearton, S.J., Ren, F., 2011. Circular and rectangular via holes formed in SiC via using ArF based UV excimer laser. Applied Surface Science 257, 2303–2307.
Liu, K., Li, X., Liang, S.Y., Liu, X.D., 2005. Nanometer-scale, ductile-mode cutting of soda-lime glass. Journal of Manufacturing Processes 7, 95–101.
Matsumura, T., Ono, T., 2008. Cutting process of glass with inclined ball end mill. Journal of Materials Processing Technology 200, 356–363.
Moriwaki, T., Shamoto, E., Inoue, K., 1992. Ultraprecision ductile cutting of glass by applying ultrasonic vibration. CIRP Annals - Manufacturing Technology 41, 141–144.
Park, Y.S., 1998. SiC Materials and Devices. Academic Press, p. 20.
Seward III, T.P., Vascott, T., 2005. High Temperature Glass Melt Property Database for Process Modeling. The American Ceramic Society, Ohio.
Toshiba, 2011. www.toshiba-machine.co.jp/english/product/high/contents/molding02.html.
Tsai, Y.C., Hung, C.H., Hung, J.C., 2008. Glass material model for the forming stage of the glass molding process. Journal of Materials Processing Technology 201, 751–754.
Yan, J., Oowada, T., Zhou, T., Kuriyagawa, T., 2009. Precision machining of microstructures on electroless-plated NiP surface for molding glass components. Journal of Materials Processing Technology 209, 4802–4808.
Yang, W.H., Tarng, Y.S., 1998. Design optimization of cutting parameters for turning operations based on the Taguchi method. Journal of Materials Processing Technology 84, 122–129.
Yuen, P.K., Kricka, L.J., Wilding, P., 2000. Semi-disposable microvalves for use with microfabricated devices or microchips. Journal of Micromechanics and Microengineering 10, 401.
Zhou, T., Yan, J., Yoshihara, N., Kuriyagawa, T., 2010. Study on nonisothermal glass molding press for aspherical lens. Journal of Advanced Mechanical Design, Systems, and Manufacturing 4, 806–815.